Structure and Rotational Dynamics of Fluorescently Labeled Insulin in Aqueous Solution and at the Amphiphile−Water Interface of Reversed Micelles†

Volker J. Lenz,*,‡ Matthias Federwisch,§ Hans-Gregor Gattner,‡ Dietrich Brandenburg,‡ Hartwig Höcker,‡ Ulrich Hassiepen,§ and Axel Wollmer§

Deutsches Wollforschungsinstitut an der Rheinisch-Westfälischen Technischen Hochschule Aachen, Veltmanplatz 8, 52062 Aachen, Germany, and Institut für Biochemie, Klinikum der Rheinisch-Westfälischen Technischen Hochschule Aachen, Pauwelsstrasse 30, 52057 Aachen, Germany

Received October 10, 1994; Revised Manuscript Received February 10, 1995⊗

ABSTRACT: Insulin is a proteohormone with amphipathic three-dimensional structure and the ligand of a receptor, which itself spans the plasma membrane of glucose-metabolizing cells. In this study, the possible impact of amphiphiles on structural and dynamic properties of the hormone was investigated in reversed micelles mimicking the amphipathic nature of biological membranes. To make insulin susceptible to fluorescence measurements, two derivatives labeled with 2-aminobenzoic acid (Abz), $N^{\epsilon B29}$-Abz-insulin and [Abz^{B1}]insulin, were prepared. First, the Abz-labeled insulins were shown by CD spectroscopy to exhibit conformational properties and self-association as well as the T→R transition similar to the native hormone. By means of time-resolved fluorescence measurements, not only metal-ion induced hexamerization was observable in aqueous solution: The T→R allosteric transition of the hexamer was shown to be accompanied by a diminution of its hydrodynamic radius. Second, structure and rotational dynamics of the labeled insulins were investigated in reversed micelles. In sodium bis(2-ethylhexyl)sulfosuccinate (AOT) reversed micelles, the main-chain conformation is similar to that in aqueous solution according to CD spectroscopy in the far-UV, whereas the weak circular dichroism in the near-UV is indicative of reduced aromatic contacts as well as of the absence of quaternary structure, and the CD spectra show the same shape as found for proteins in an intermediate state of folding referred to as the "molten globule". Fluorescence anisotropy decay measurements of $N^{\epsilon B29}$-Abz-insulin in reversed micelles of AOT, cetyltrimethylammonium bromide, and α-L-1,2-dioctanoylphosphatidylcholine showed that the internal mobility of the solubilizate is reduced compared to that in aqueous solution and that the rotational mobility of the labeled insulin decreases with decreasing micellar size. With respect to the immobilization, insulin interacts in a stronger way with the anionic than with the cationic or zwitterionic amphiphile; an integration into the amphiphile monolayer, however, could be ruled out in all cases. In conclusion, the results reveal an evident influence of amphiphiles on the structure and rotational dynamics of insulin. Further investigations should be focused on this finding also with regard to the possible importance of lipid−insulin interactions in vivo.

In biological systems, the structure and function of proteins are often influenced by the interaction with lipids of the plasma membrane or intracellular membranes; the membranes themselves are functionalized by the presence of proteins (Chapman et al., 1979). While intensive studies on the properties of typical membrane proteins answered questions about structural and topological aspects in some cases, only in the near past, a novel model was proposed which takes lipid−protein interactions into consideration for the regulation of the physiological function of biologically active peptides and proteohormones being ligands of membrane-integral receptors: Sargent and Schwyzer (1986) extended the traditional concept of a direct, one-step ligand−receptor interaction to a model which is based on several sequential steps, such as ligand accumulation on the membrane surface, formation of a conformation or orientation favorable for the interaction with the receptor as a consequence of lipid−protein interactions, and finally the ligation of the receptor. On the basis of this concept, frequently occurring phenomena as, e.g., high apparent association constants of ligands, the heterogeneity of receptor binding sites, and different binding characteristics of cells originating from different tissues can be explained.

To take the conditions in biological systems experimentally into account, an increasing number of investigations on interactions between amphiphilic molecules, forming microstructured self-assemblies, with proteins have been performed (Fendler, 1982). These microstructured systems are used as model membranes for treating the following problems: Under which conditions do amphiphile−protein interactions occur? What is the nature of these interactions? To what extent are the structure and function of the proteins altered? This complex of questions links up aspects of supramolecular chemistry with supramolecular properties of biological systems (Ringsdorf et al., 1988; Ahlers et al., 1990).

† This work was supported by a grant from the Deutsche Forschungsgemeinschaft.

* To whom correspondence should be addressed. Telefax: +241/4469-100.

‡ Deutsches Wollforschungsinstitut.

§ Institut für Biochemie.

⊗ Abstract published in *Advance ACS Abstracts,* April 15, 1995.

0006-2960/95/0434-6130$09.00/0

Since insulin is a molecule with amphipathic structure, which is also responsible for its self-association in solution, and since it is a ligand of a transmembrane receptor, the question should be taken into account of whether lipid−insulin interactions are also of importance to the in vivo mechanism of insulin action. On the other hand, not much is known about the specificity of lipid−protein interactions and the consequences to structural and dynamic properties of interacting proteins. In the special case of insulin, information on the impact of lipids on its conformation and quarternary structure as well as on specific interactions with lipids is particularly sparse (Wu & Yang, 1981). With respect to the structural variability of insulin hexamers (Renscheidt et al., 1984; Wollmer et al., 1987) and of monomeric insulin in solution, which is in the latter case viewed as an ensemble of closely related conformers (Hua et al., 1992a), lipid−insulin interactions could be relevant to stabilize a particular conformation in vivo, for instance after accumulation at the cell surface. Thereby, the specificity of membrane−insulin interactions could be controled by the lipid pattern of the plasma membrane.

Against this background, Sackmann and his group have shown specific and nonspecific binding of fluorescein-labeled insulin to supported membranes of phospholipids, but the influence of the artificial membranes on the structure and dynamics of the hormone was not enquired into (Sui et al., 1988). To investigate these aspects of lipid−insulin interactions, we used reversed micelles mimicking the amphipathic nature of biological membranes. Reversed micelles are self-organized assemblies of amphiphiles, thermodynamically stable in organic solvents and in the presence of limited amounts of water (Eicke, 1980). Such micelles are designated as reversed since the polar amphiphile head groups are directed to the aqueous interior of these spheroidal aggregates, while their hydrocarbon tails protrude into the apolar bulk solvent. The key structural parameter of the reversed micelle is the water/amphiphile molar ratio, w_0 = [water]/[amphiphile], which determines the micellar size as well as the special physicochemical properties of the entrapped water. Different species of water molecules are found in reversed micelles, immobilized ones at the amphiphile−water interface and more mobile ones in the center of the micelle with an exchange between the respective populations. Water molecules bound to the amphiphile head groups were found to be of lower polarity than of bulk water (Menger et al., 1973). Reversed micelles are advantageous compared to other membrane mimetic systems because their simple microstructure allows a detailed investigation of interactions of solubilizates with amphiphile monolayers at the water−amphiphile interface by varying the charge and solvation state of the amphiphile head groups (Nicot et al., 1985).

In order to make insulin susceptible to fluorescence spectroscopic studies in reversed micelles, we prepared insulins covalently conjugated with 2-aminobenzoic acid (Abz)[1] (Haugland & Stryer, 1967). The intrinsic fluorescence of native insulin is very low, and the high number of tyrosine residues, especially in the hexameric state, precludes a resolution of the fluorescence of this multifluorophore system (Federwisch, 1993). In contrast to this, the Abz fluorophore allows a selective excitation outside the spectral region of protein absorption; furthermore, its spectral properties are sensitive to solvent polarity and molecular environment. We show by CD spectroscopy that the solution structure of the labeled insulins is not altered compared to the native hormone. By means of time-resolved fluorescence measurements, the hydrodynamic parameters are determined in different states of self-association. After proof of the persistence of the native-like structure in aqueous solution as well as of the hormonal properties in vitro, conformation, quaternary interactions, and rotational dynamics are investigated in reversed micelles as a function of the water/amphiphile molar ratio and the charge of the head groups of the amphiphiles AOT, CTAB, and DOcPC used as solubilization mediators.

MATERIALS AND METHODS

Materials. 2-Aminobenzoic acid and DCC were purchased from Merck AG (Darmstadt, Germany). AOT was purchased from Aldrich (Steinheim, Germany) and purified as described by Martin and Magid (1981), CTAB was from Serva (Heidelberg, Germany; purified by 2-fold recrystallization from methanol), and DOcPC was from Sigma (Deisenhofen, Germany; used without further purification). Porcine insulin was a generous gift of Dr. Obermeier, Hoechst AG (Frankfurt, Germany).

Analytical and Chromatographic Methods. Gel filtrations were performed on Sephadex G-25 fine or G-50 fine from Pharmacia (Uppsala, Sweden), and ion-exchange chromatography on SP-TSK-Fractogel and DEAE-TSK-Fractogel from Merck AG. At pH 2.7, a 1.5 M solution of acetic acid in 2-propanol/water (2/3; v/v) and, at pH 7.2, a 0.02 M Tris/HCl buffer in 2-propanol/water (2/3; v/v) were used for ion-exchange chromatography. The RP_{18}-silica gel was a gift of Dr. Behn, Abimed (Langenfeld, Germany). All elutions were performed in a linear gradient mode. For analytical RP-HPLC, the liquid chromatograph LC 41 D/CD from Bruker-Franzen Analytik (Bremen, Germany) was used. A 0.025 M H_3PO_4/Et_3N buffer, pH 2.25, and a linear acetonitrile gradient were used for elution on a Nucleosil 100−5 C18 RP-column. To check the purity of insulin derivatives, an elution program using a gradient from 20 to 50 vol % acetonitrile in 30 min was performed. Capillary zone electrophoreses were performed on a Bio-Rad HPE 100 or a Biofocus 3000 capillary electrophoresis system using coated capillaries (length = 24 cm, diameter = 25 μm) in 0.1 M aqueous NaH_2PO_4/H_3PO_4, pH 2.5.

For amino acid analyses (Spackman et al., 1958) on Model LC 5000 from Biotronic (München, Germany), insulin

[1] Abbreviations: Abz, 2-aminobenzoic acid; AOT, sodium bis(2-ethylhexyl)sulfosuccinate; β, content of β-structure; Boc, *tert*-butyloxycarbonyl; CD, circular dichroism; CTAB, cetyltrimethylammonium bromide; DCC, *N,N'*-dicyclohexylcarbodiimide; CZE, capillary zone electrophoresis; DCU, *N,N'*-dicyclohexylurea; DEAE, diethylaminoethyl; DMF, *N,N*-dimethylformamide; DMSO, dimethyl sulfoxide; DOcPC, α-L-1,2-dioctanoylphosphatidylcholine; Et, ethyl; FAD, fluorescence anisotropy decay; *H*, α-helix content; HPLC, high-performance liquid chromatography; MRW, mean residue weight; Msc, methylsulfonylethoxycarbonyl; NMM, *N*-methylmorpholine; *i*-octane, 2,2,4-trimethylpentane; NOESY, two-dimensional nuclear Overhauser enhancement spectroscopy; ONSu, succinimidooxy; *R*, remainder of nonperiodic structure; R_6, structure of the insulin hexamer in monoclinic 2Zn crystals; RP, reversed phase; SP, sulfopropyl; st, indication that a pH value is related to a stock solution before solubilization in a reversed micellar system; *T*, content of the structural element β-turn; T_6, structure of the insulin hexamer in rhombohedral 2Zn crystals; Tris, tris(hydroxymethyl)aminomethane; wp, indication that a concentration is related to micellar water.

derivatives were hydrolyzed in 6 M aqueous HCl in the presence of phenol for 24 h at 110 °C; in separate experiments, it was shown that 2-aminobenzoic acid is destroyed under these conditions. For amino end-group determination, the proteins were dansylated with dansyl chloride (Gray & Hartley, 1963). After hydrolysis of the dansylated protein for 9 h at 110 °C, the dansyl amino acids were identified by RP-HPLC analysis using dansylation products of proteinogenic amino acids and 2-aminobenzoic acid as references. Although *N*-dansyl-2-aminobenzoic acid was destroyed under the acidic conditions used, its presence and position could be determined indirectly by inspection of the dansyl amino acid pattern of the insulin derivatives.

For the determination of water in reversed micellar solutions, the Karl-Fischer coulometer 684 without diaphragm from Metrohm AG (Herisau, Switzerland) and the reagent HYDRANAL Coulomat AD from Riedel-de Haen (Seelze, Germany) were used.

Preparation of N-Boc-(2-aminobenzoic acid). 2-Aminobenzoic acid was protected by the Boc group similar to the general procedure described in the literature (Moroder et al., 1976), mp 151−152 °C.

Preparation of $N^{\epsilon B29}$-Abz-Insulin. Boc-Abz (59 mg, 0.249 mmol) was preactivated by reaction with HOBt (33 mg, 0.244 mmol) and DCC (46 mg, 0.223 mmol) in 0.5 mL of DMF for 45 min at room temperature. Then the precipitated DCU was separated by centrifugation, and the supernatant was added to a solution of $N^{\alpha A1}$,$N^{\alpha B1}$-bis(Msc)insulin (300 mg, 0.049 mmol), prepared according to Schüttler (1979), in 10 mL of DMF containing 0.1 mL of NMM. After being stirred for 1.5 h, the acylation was stopped by addition of 15 mL of 10 vol % aqueous acetic acid under cooling. Excess carboxy component was separated by gel filtration on Sephadex G-25. The fraction containing $N^{\epsilon B29}$-(Boc-Abz)-$N^{\alpha A1}$,$N^{\alpha B1}$-bis(Msc)insulin was lyophilized, yield 267 mg.

The Msc groups were removed by addition of 3 mL of 2 M aqueous NaOH to a solution of the fully N-protected insulin derivative in 20 mL of 1,4-dioxane/water (1/1; v/v) at 0 °C. After 70 s, the solution was acidified by addition of 3 mL of glacial acetic acid under stirring. 1,4-Dioxane was removed under reduced pressure, and gel chromatography on Sephadex G-50 was performed. $N^{\epsilon B29}$-(Boc-Abz)-insulin was purified by chromatography on RP_{18}-silica gel; gradient elution was performed with 20−40 vol % 2-propanol in 0.1 vol % aqueous trifluoroacetic acid and yielded 168 mg of lyophilized material.

Finally, the Boc group was removed in 5 mL of trifluoroacetic acid for 45 min at room temperature. The solution then was poured into 30 mL of diethyl ether, and the precipitate was separated by centrifugation and decantation. The dried material was chromatographed on Sephadex G-25 and purified by ion-exchange chromatography on SP-Fractogel (pH 2.7; 600 mL of starting buffer, 600 mL of buffer containing 0.1 M NaCl as gradient) and on DEAE-Fractogel (pH 7.3; 500 mL of starting buffer, 500 mL of buffer containing 0.08 M NaCl as gradient). After gel filtration on Sephadex G-25, the product was lyophilized: yield, 44 mg [15% based on $N^{\alpha A1}$,$N^{\alpha B1}$-bis(Msc)insulin]; RP-HPLC purity, 98%; CZE purity, 96%; dansylamino acids, dansyl-Gly, dansyl-Phe, *O*-dansyl-Tyr; amino acid analysis (theoretical values in parentheses), Asp 2.98 (3), Thr 1.67 (2), Ser 2.77 (3), Glu 7.00 (7), Pro − (not determined), Gly 4.04 (4), Ala 2.00 (2), Val 3.36 (4), $(Cys)_2$ 2.34 (3), Ile 1.36 (2), Leu 6.00 (6), Tyr 3.72 (4), Phe 2.69 (3), Lys 1.00 (1), His 1.87 (2), Arg 0.99 (1).

Preparation of [Abz^{B1}]Insulin. Boc-Abz (40 mg, 0.169 mmol) was preactivated by reaction with HOBt (23 mg, 0.170 mmol) and DCC (31 mg, 0.150 mmol) in 0.5 mL of DMF for 45 min at room temperature. Then the precipitated DCU was separated by centrifugation, and the supernatant was added to a solution of $N^{\alpha A1}$,$N^{\epsilon B29}$-bis(Msc)des-Phe^{B1}-insulin (200 mg, 0.033 mmol), prepared according to Geiger et al. (1975), in 10 mL of DMF containing 0.1 mL of NMM. After being stirred for 1.5 h, the acylation was stopped by addition of 15 mL of 10 vol % aqueous acetic acid under cooling. Excess carboxy component was separated by gel filtration on Sephadex G-25. The fraction containing N^{B1}-Boc-$N^{\alpha A1}$,$N^{\epsilon B29}$-bis(Msc)[Abz^{B1}]insulin was collected and lyophilized. The crude material was purified by chromatography on RP_{18}-silica gel; gradient elution was performed with 20−40 vol % 2-propanol in 0.1 vol % aqueous trifluoroacetic acid, yield after lyophilization 123 mg.

The Msc groups were removed as described above, but without further purification, yield 94 mg.

After treatment with trifluoroacetic acid, the completely deprotected product was finally purified by ion-exchange chromatography on SP-Fractogel (pH 2.7; 500 mL of starting buffer, 500 mL of buffer containing 0.15 M NaCl as gradient) and on DEAE-Fractogel (pH 7.3; 500 mL of starting buffer, 500 mL of buffer containing 0.1 M NaCl as gradient). After gel filtration on Sephadex G-25 the product was lyophilized: yield, 44 mg [23% based on $N^{\alpha A1}$,$N^{\epsilon B29}$-bis-(Msc)des-Phe^{B1}-insulin]: RP-HPLC purity, 95%; CZE purity, 99%; dansylamino acids, dansyl-Gly, *N*-dansyl-Lys, *O*-dansyl-Tyr; amino acid analysis (theoretical values in parentheses), Asp 3.00 (3), Thr 1.76 (2), Ser 2.56 (3), Glu 7.04 (7), Pro 0.98 (1), Gly 3.96 (4), Ala 1.92 (2), Val 3.29 (4), $(Cys)_2$ 2.36 (3), Ile 1.31 (2), Leu 6.00 (6), Tyr 3.68 (4), Phe 2.03 (2), Lys 0.97 (1), His 1.98 (2), Arg 0.95 (1).

Bioassays. Lipogenesis was measured by the method according to Moody et al. (1974). Biological potencies were calculated from the linear portion of the logarithmic dose−response curves using parallel-line bioassay techniques (Finney, 1964). The assay of De Meyts (1976) was used to determine relative binding to cultured human IM-9 lymphocytes. The concentrations were based on weight. Identical solutions were used for both potency and binding assays. The values are given as means of triple determinations relative to native insulin ± standard deviation from the mean.

Preparation of Aqueous Solutions. The insulin derivatives were dissolved in 25 mM Tris/HCl buffer, pH 7.8. Concentrations were determined photometrically using a Pye-Unicam PU 8800 UV/VIS spectrophotometer from Philips (Kassel, Germany). The molar extinction coefficients used are $\epsilon_{276} = 7090\ M^{-1}\ cm^{-1}$ for $N^{\epsilon B29}$-Abz-insulin, $\epsilon_{276} = 6480\ M^{-1}\ cm^{-1}$ for [Abz^{B1}]insulin based on quantitative amino acid analysis as described earlier (Lenz et al., 1994), and $\epsilon_{276} = 6066\ M^{-1}\ cm^{-1}$ for native porcine insulin (Frank & Veros, 1968). For fluorescence measurements, the optical density was ≤0.1 at the wavelength of excitation in all cases. All measurements were carried out at 22 °C.

Preparation of Reversed Micellar Solutions. Reversed micellar solutions were prepared by the injection method or by direct solubilization of the lyophilized protein in the reversed micellar solvent system (Luisi, 1985). Protein

concentrations are usually given as overall concentrations; the subscript "wp" indicates that a concentration is related to the volume of the solubilized water. The following multicomponent systems were used: AOT (0.05 M)/*i*-octane/water, CTAB (0.05 M)/*i*-octane/trichloromethane (1/1; v/v)/water, and DOcPC (50 mM)/*i*-octane/hexanol (9/1; v/v)/water. In all cases, water was buffered with 25 mM Tris/HCl at pH 7.8, and protein concentrations were determined photometrically using the molar extinction coefficients measured in aqueous solution. After solubilization of the proteins, the water concentration of the solvent systems was determined by coulometric Karl–Fischer titration.

Circular Dichroism. CD measurements were carried out on an AVIV (Lakewood, NJ) 62 DS CD spectrometer calibrated with a 0.1% aqueous solution of *d*-10-camphorsulfonic acid according to Chen and Yang (1977). Further details were described earlier (Renscheidt et al., 1984). To determine the secondary structural composition, the spectra were analyzed with the CONTIN (Provencher & Glöckner, 1981) and the VARSELEC (Johnson, 1990) program package.

Fluorescence Measurements. Steady-state fluorescence spectra were recorded on a Perkin-Elmer LS 50 luminescence spectrometer (Bodenseewerk, Germany) and on a Spex Fluorolog 211 photon counting spectrofluorometer (Spex Industries, New York, NY). Steady-state emission maxima were reproducible within an error range of 0.5 nm. Time-resolved fluorescence intensity and fluorescence anisotropy decay were measured in the single photon counting mode with an Edinburgh Instruments Ltd. (U.K.) spectrometer, Model 199. The Abz fluorophore was excited at 330 nm. Its emission was passed through a KV 380 cutoff filter supplied by Schott (Mainz, Germany). The lamp pulse was recorded at 410 nm. Depending on the available intensity, the bandwidth of the excitation monochromator was varied between 4 and 16 nm. Cumulation was stopped when at least 60 000 counts were stored in the peak channel for the total fluorescence intensity decay. The data handling and the iterative nonlinear least-squares fit of the decays were accomplished with a program supplied by Edinburgh Instruments Ltd.: The standard deviations of τ_i and ϕ_i given by the program and listed in the tables are purely statistical in origin and cannot be directly equated to parameter errors, because they take no account of parameter correlations or systematic errors. They are calculated on the basis of error of the mean. The quality of fits was judged by the reduced chi-squared, χ^2. The weighted residuals were checked for random distribution (Szabo & Rayner, 1980). The analyses of the time-resolved measurements were performed as described previously (Federwisch et al., 1992).

RESULTS

Biological in Vitro Properties. Biological potency and receptor binding of the Abz-labeled insulins relative to porcine insulin were determined in vitro: The values obtained are 81% ± 9% and 60% ± 4% for $N^{\epsilon B29}$-Abz-insulin, 113% ± 15% and 160% ± 10% for [Abz^{B1}]insulin, respectively.

CD Measurements in Aqueous Solution. Figure 1 shows the far-UV CD spectra of $N^{\epsilon B29}$-Abz-insulin, [Abz^{B1}]insulin, and porcine insulin at concentrations where monomers are forming a substantial fraction of the monomer–oligomer

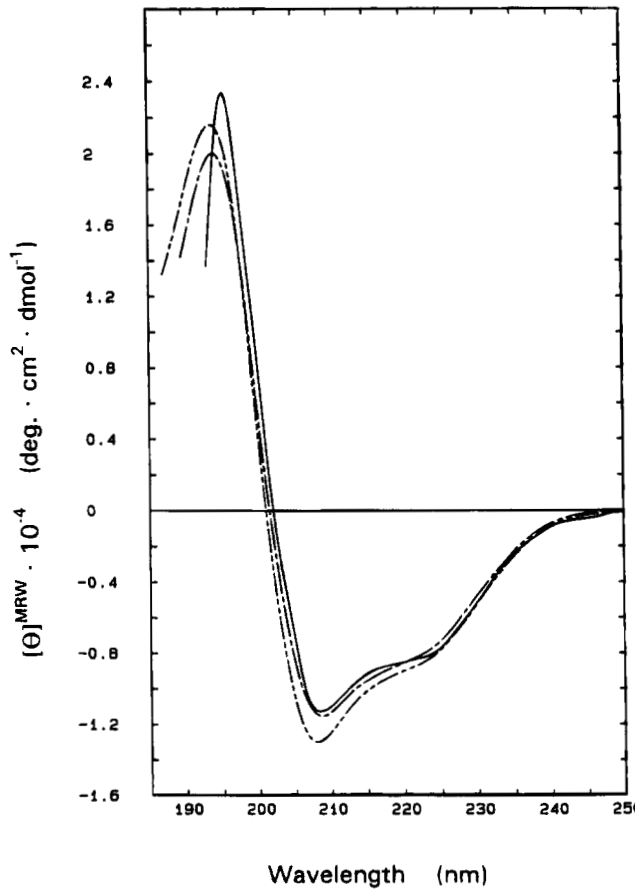

FIGURE 1: Far-UV CD spectra of porcine insulin, $N^{\epsilon B29}$-Abz-insulin, and [Abz^{B1}]insulin at monomer concentration in 5 mM aqueous sodium phosphate buffer, pH 7.8. (—) 3.5 μM porcine insulin; (– – –) 2.0 μM $N^{\epsilon B29}$-Abz-insulin; (– – –) 3.4 μM [Abz^{B1}]insulin.

equilibrium (Wood et al., 1975). The spectra are similar in shape and suggest that the main-chain conformations of insulin and the labeled species are nearly the same. In spite of the inherent achirality of the Abz chromophore, the near-UV spectra of both Abz-labeled insulins exhibit negative extrinsic Cotton effects around 330 nm additional to the tyrosyl CD of native insulin, and the CD spectrum of [Abz^{B1}]-insulin (Figure 2) shows a further negative band at 258 nm which is also due to an electronic transition of the aromatic amine (Doub & Vandenbelt, 1949). Upon increasing the protein concentration and adding Zn^{2+} ions, the CD spectral changes in the near-UV as well as in the far-UV range (not depicted) of both labeled insulins correspond to the association behavior known from the native hormone (Wood et al., 1975). Furthermore, not only the metal-ion-induced formation of hexamers but also the $T_6 \rightarrow R_6$ allosteric transition in the presence of phenol [Wollmer et al., 1987; for terminology, see Derewenda et al. (1989) and Kaarsholm et al. (1989)] are accompanied by a significant increase of the negative ellipticity in the near-UV range.

Steady-State and Time-Resolved Fluorescence Measurements in Aqueous Solution. The emission spectra of $N^{\epsilon B29}$-Abz-insulin and [Abz^{B1}]insulin in aqueous solution are nearly identical in shape and intensity. Upon excitation at 330 nm, the spectra exhibit emission maxima at 415 and 416 nm, respectively. Neither formation of the hexamer nor the T→R structural transition significantly affects the emission spectra.

The results of the time-resolved measurements of the fluorescence intensity are summarized in Table 1. None of

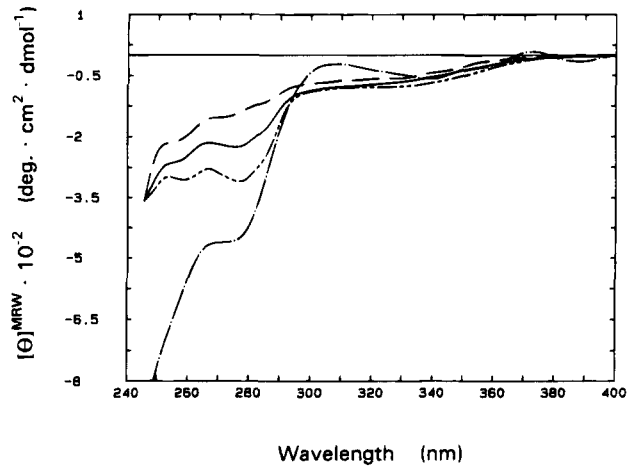

FIGURE 2: Near-UV CD spectra of [Abz^{B1}]insulin with increasing concentration, upon addition of Zn^{2+} ions, and after phenol-induced transformation to the R_6 state in aqueous buffer, pH 7.8. (— —) 3.4 μM; (—) 172 μM; (— - - —) 169 μM, 0.33 equiv of Zn^{2+}/monomer; (— • —) 169 μM, 0.33 equiv of Zn^{2+}/monomer, and 16.3 mM phenol.

Table 1: Fluorescence Intensity Decay Parameters of (1−3) $N^{\epsilon B29}$-Abz-Insulin and (4−6) [Abz^{B1}]Insulin in Different Association States in Aqueous 25 mM Tris Buffer, pH 7.8[a]

	B_1	B_2	B_3	τ_1 (ns)	τ_2 (ns)	τ_3 (ns)	$\langle\tau\rangle$ (ns)	χ^2
(1)	0.02	0.64	0.34	1.10 ± 0.19	7.30 ± 0.14	11.27 ± 0.08	8.5	1.07
(2)	0.03	0.83	0.14	2.25 ± 0.33	8.52 ± 0.12	13.49 ± 0.17	9.0	1.07
(3)	0.02	0.48	0.50	2.20 ± 0.61	7.66 ± 0.30	10.79 ± 0.06	9.1	1.03
(4)	0.02	0.21	0.77	1.05 ± 0.14	6.22 ± 0.39	9.47 ± 0.03	8.6	1.13
(5)	0.11	0.89		3.84 ± 0.13	9.18 ± 0.01		8.6	1.11
(6)	0.05	0.95		3.35 ± 0.22	9.40 ± 0.01		9.1	1.13

[a] (1) 3 μM $N^{\epsilon B29}$-Abz-insulin; (2) 170 μM $N^{\epsilon B29}$-Abz-insulin, 0.33 equiv of Zn^{2+}/monomer; (3) 170 μM $N^{\epsilon B29}$-Abz-insulin, 0.33 equiv of Zn^{2+}/monomer, 16.3 mM phenol; (4) 4 μM [Abz^{B1}]insulin; (5) 174 μM [Abz^{B1}]insulin, 0.33 equiv of Zn^{2+}/monomer; (6) 174 μM [Abz^{B1}]insulin, 0.33 equiv of Zn^{2+}, 16.3 mM phenol. Temperature: 22 °C. Excitation wavelength was 330 nm, bandwidth 16 nm and 4 nm for the monomer and hexamer, respectively, filter KV 380; the lamp pulse was recorded at 410 nm. The fits of the data are based on the equation $S(t) = a_0 + \sum a_i \exp(-t/\tau_i)$ with $i = 1, \ldots n$ which describes the rotation-free total intensity decay. a_0 represents the background of the dark counting noise of the instrument; a_i and τ_i are the amplitude and lifetime of the ith excited state, respectively. The standard deviations of τ_i given in the table are explained under Materials and Methods. B_i and the average fluorescence decay time, $\langle\tau\rangle$, were calculated according to $\langle\tau\rangle = \sum B_i\tau_i = \sum a_i\tau_i^2/\sum a_i\tau_i$ (Inokuti & Hirayama, 1965) and rounded off.

the fluorescence intensity decays of the labeled insulins is monoexponential. According to χ^2 optimization and deviation function criteria, a triexponential model improves the fit of the experimental data (Figure 3). However, two lifetimes are sufficient to fit the total intensity decay of [Abz^{B1}]insulin under hexameric conditions (see Table 1). The mean fluorescence lifetimes, $\langle\tau\rangle$, of $N^{\epsilon B29}$-Abz-insulin and [Abz^{B1}]insulin in the monomeric state are 8.5 and 8.6 ns, respectively. These values are coincident with the results of Chen et al. (1967), who reported a mean lifetime of 8.4 ± 0.5 ns for 2-aminobenzoic acid in aqueous solution. When going from the monomeric state to the hexameric T and R states, the mean lifetime only slightly increases, which is in line with the nearly unchanged steady-state emission spectra.

The increase of the hydrodynamic radii of $N^{\epsilon B29}$-Abz-insulin and [Abz^{B1}]insulin in different association states could be followed by FAD measurements (Table 2), and the

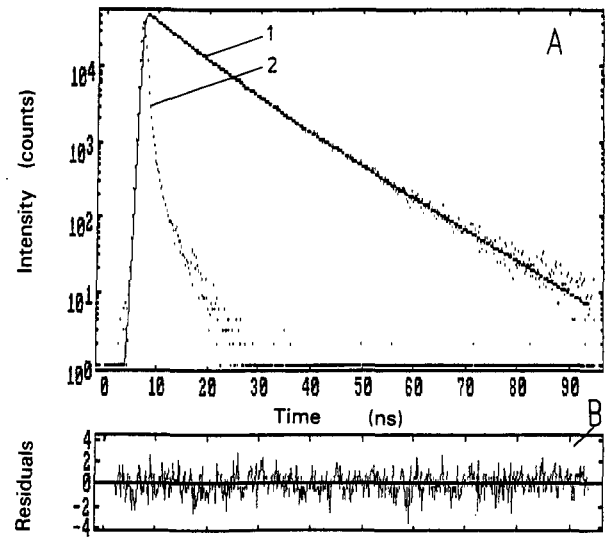

FIGURE 3: (A) Fluorescence intensity decay of monomeric $N^{\epsilon B29}$-Abz-insulin in aqueous 25 mM Tris buffer at pH 7.8 (1), curve fitting based on a triexponential model (line), and lamp pulse at 410 nm (2). (B) Residuals. 3.0 μM $N^{\epsilon B29}$-Abz-insulin; excitation at 330 nm, spectral bandwidth 16 nm; emission filter KV 380. $\langle\tau\rangle$ = 8.5 ns, χ^2 = 1.07. For further parameters, see Table 1.

Table 2: Fluorescence Anisotropy Decay Parameters of (1−3) $N^{\epsilon B29}$-Abz-Insulin and (4−6) [Abz^{B1}]Insulin in Different Association States in Aqueous 25 mM Tris Buffer, pH 7.8[a]

	r_0	r_1	r_2	r_∞	ϕ_1 (ns)	ϕ_2 (ns)	χ^2	α
(1)	0.204	0.190		0.014	2.3 ± 0.1		0.91	
(2)	0.239	0.095	0.126	0.018	1.3 ± 0.3	10.8 ± 0.8	1.11	0.40
(3)	0.266	0.089	0.157	0.020	1.0 ± 0.2	9.6 ± 0.4	1.04	0.33
(4)	0.223	0.204		0.019	2.5 ± 0.1		1.89	
(5)	0.317	0.059	0.250	0.008	1.0 ± 0.2	14.5 ± 0.6	1.02	0.19
(6)	0.311	0.036	0.258	0.017	1.0 ± 0.3	12.0 ± 0.4	0.91	0.12

[a] For concentrations and experimental conditions, see footnote to Table 1. r_i are the fitted anisotropies and ϕ_i the rotational correlation times based on the equation $r(t) = \sum r_i \exp(-t/\phi_i) + r_\infty$, with $i = 1, 2$. The standard deviations of ϕ_i given in the table are explained under Materials and Methods. The limiting anisotropies are: $r(t\rightarrow 0) = r_0$, $r(t\rightarrow\infty) = r_\infty$, with $r_0 = r_1 + r_2 + r_\infty$. α is defined as the ratio r_1/r_0 (Lakowicz, 1986).

limiting anisotropies, r_0, were found to be in accordance with the value of r_0 = 0.304 reported by Haugland and Stryer (1967). In the monomeric state, analysis of the FAD measurements by a monoexponential model (Figure 4) results in rotational correlation times of 2.3 and 2.5 ns. Under hexameric conditions, the anisotropy decay has throughout to be fitted with two exponentials to improve χ^2, and the metal-ion-induced hexamerization of both labeled insulins is reflected in an increase of the long correlation time ϕ_2 to 10.8 and 14.5 ns, respectively. The $N^{\epsilon B29}$-Abz-insulin hexamer shows a significantly higher α than [Abz^{B1}]insulin under hexameric conditions. α is defined as the ratio r_1/r_0 and was introduced by Lakowicz (1986) as a criterion for the side-chain mobility or segmental flexibility of a protein: The lower α, the higher the rigidity of the side chain or the segment is. Furthermore, the transition from the T_6 to the R_6 state induced by phenol is accompanied by a decrease of ϕ_2 and α of both derivatives.

CD Measurements in Reversed Micelles and Numerical Analysis of Secondary Structure. Because of the low transparency of the solvent systems containing hexanol as cosolvent, CD spectroscopic investigations were performed

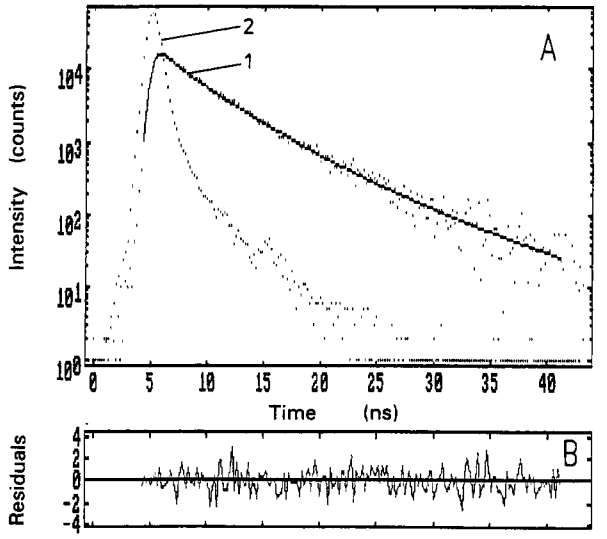

FIGURE 4: (A) Decay of the difference between vertical and horizontal polarization of monomeric $N^{\epsilon B29}$-Abz-insulin in aqueous 25 mM Tris buffer at pH 7.8 (1), curve fitting based on a monoexponential model (line), and lamp pulse at 410 nm (2). (B) Residuals. 3.0 μM $N^{\epsilon B29}$-Abz-insulin; excitation at 330 nm; spectral bandwidth 16 nm; emission filter KV 380. $r_0 = 0.204$, $r_1 = 0.190$, $\phi_1 = 2.3$ ns, $\chi^2 = 0.91$.

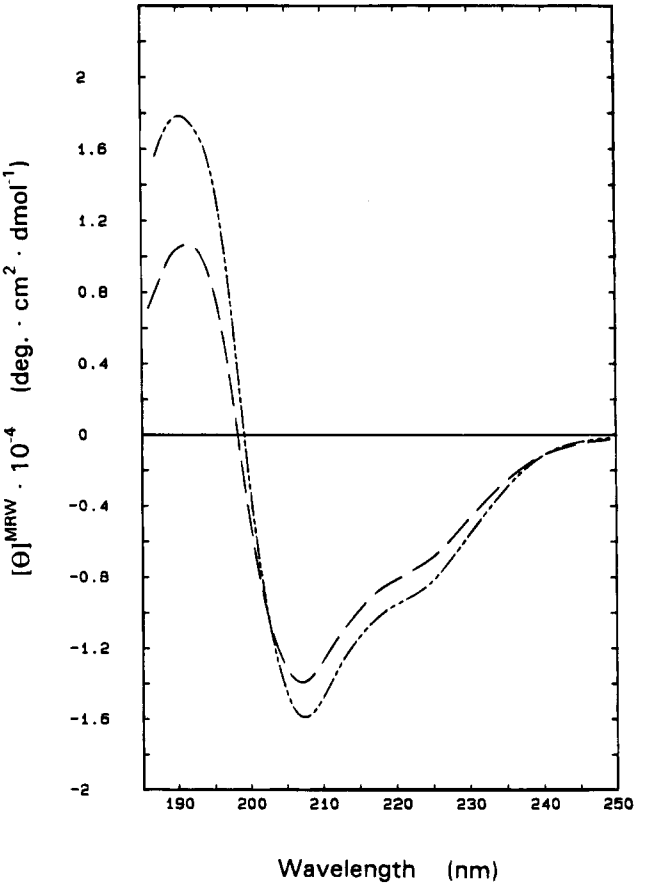

FIGURE 5: Far-UV CD spectra of $N^{\epsilon 29}$-Abz-insulin in AOT (0.05 M)/*i*-octane/water, 25 mM_{wp} Tris, pH_{st} 7.8, at different water/AOT ratios. (- - -) $w_0 = 9$, 100 μM $N^{\epsilon B29}$-Abz-insulin; (— —) $w_0 =$ 35, 95 μM $N^{\epsilon B29}$-Abz-insulin.

exclusively on the system AOT/*i*-octane. In Figure 5, the far-UV CD spectra of $N^{\epsilon B29}$-Abz-insulin in AOT micelles at w_0 values of 9 and 35 are depicted. The overall ellipticity in the far-UV range decreases with increasing micellar size.

Table 3: Results of the Numerical Analyses of the Far-UV CD Spectra of Porcine Insulin and Abz-Labeled Insulins According to the Method of (P) Provencher and Glöckner (1981) and (J) Johnson (1990), Respectively[a]

protein	concn (μM)	method	w_0	H (%)	β (%)	T (%)	R (%)
insulin	80	P	9	39	18	21	22
	95	P	35	31	20	23	26
	80	J	9	39	21	20	16
	95	J	35	32	20	25	19
$N^{\epsilon B29}$-Abz-insulin	100	P	9	37	19	21	23
	95	P	35	31	20	23	26
	100	J	9	36	24	22	13
	95	J	35	32	20	25	21
[Abz^{B1}]insulin	85	P	9	38	20	20	22
	71	P	35	27	24	21	28
	85	J	9	41	21	20	15
	71	J	35	27	26	20	21

[a] Content of secondary structural elements in AOT (0.05 M)/*i*-octane/water, 25 mM_{wp} Tris, pH_{st} 7.8, at $w_0 = 9$ and $w_0 = 35$. In the method of Johnson, the fractions of main-chain conformations do not necessarily sum up to 100%.

To determine the secondary structural composition, the CD spectra were analyzed with the program packages CONTIN (Provencher & Glöckner, 1981) and VARSELEC (Johnson, 1990) using sets of reference spectra in the 185−250 nm range. The results of the analyses are summarized in Table 3, and the values of the native hormone solubilized in AOT micelles are included for comparison. Both programs, CONTIN and VARSELEC, give nearly identical results, and, according to the numerical analyses, the changes of the far-UV spectra with increasing w_0 reflect a decrease of the content of α-helical structure.

The near-UV CD spectra of native insulin (Figure 6A) as well as those of the labeled insulins in AOT micelles (Figure 6B) are substantially different from the spectra taken in aqueous solution. For native insulin, the differences, primarily the reduced band at 275 nm, point to increased dissociation in reversed micelles. Contrary to the situation in aqueous solution, the tyrosyl CD of native insulin in AOT micelles is independent of the concentration in the range $0.05 \leq$ [protein]/(mmol/L) ≤ 0.35, and the intensity and position of the bands are nearly unaffected by a variation of w_0 (Figure 6A). The CD spectrum of $N^{\epsilon B29}$-Abz-insulin reveals nearly the same shape as that of unlabeled insulin in the whole near-UV range, whereas the label in position B1 exhibits strong negative Cotton effects both at 258 nm and at 338 nm, resembling the spectral properties in aqueous solution.

Steady-State Fluorescence Spectra in Reversed Micelles. The fluorescence emission spectra of both Abz-labeled insulins were measured in reversed micelles of AOT, CTAB, and DOcPC. After solubilization at low w_0 values, the emission maxima are shifted to shorter wavelengths compared to the aqueous solution (Figure 7). This hypsochromic effect is independent of the position of the label in the molecule and corresponds to a decrease of environmental polarity. In the range $2 \leq w_0 \leq 20$, the emission maxima are shifted to longer wavelengths and become nearly identical to the maxima measured in aqueous solution at $w_0 > 20$.

Time-Resolved Fluorescence Measurements in Reversed Micelles. The results of the total fluorescence intensity decay measurements of $N^{\epsilon B29}$-Abz-insulin as a probe for insulin−amphiphile interactions in reversed micelles are given in

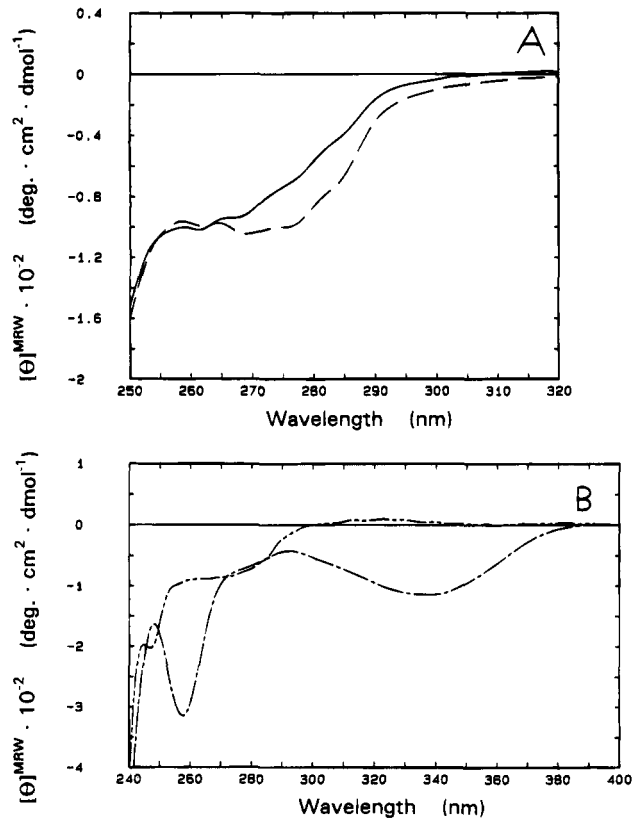

FIGURE 6: Near-UV CD spectra of (A) porcine insulin and (B) Abz-labeled insulins in AOT (0.05 M)/*i*-octane/water, 25 mM_{wp} Tris, pH_{st} 7.8. (A) (—) 83 μM insulin, $w_0 = 9$; (— —) 95 μM insulin, $w_0 = 35$. (B) (— - - —) 84 μM $N^{\epsilon B29}$-Abz-insulin, $w_0 = 9$; (— - —) 85 μM [Abz^{B1}]insulin, $w_0 = 9$.

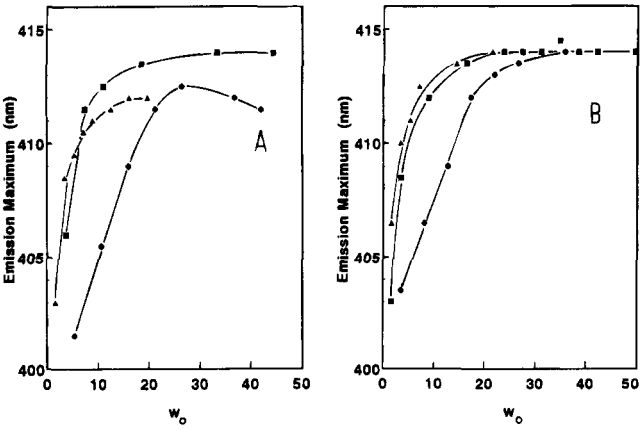

FIGURE 7: Fluorescence emission maxima of (A) $N^{\epsilon B29}$-Abz-insulin and (B) [Abz^{B1}]insulin in reversed micellar systems stabilized by amphiphiles with differently charged headgroups as a function of w_0 , 25 mM_{wp} Tris, pH_{st} 7.8. (■) AOT (0.05 M)/*i*-octane/water; (▲) CTAB (0.05 M)/*i*-octane/trichloromethane (1/1; v/v)/water; (●) DOcPC (0.05M)/*i*-octane/hexanol (9/1; v/v)/water. Excitation wavelength: 330 nm.

Table 4. The fluorescence decays reveal the same complex pattern as in aqueous solution and are best described by triple exponentials. With the exception of the DOcPC system, the mean fluorescence lifetimes slightly increase with increasing water content, but remain shorter than in aqueous solution. In DOcPC micelles, a decrease of $\langle\tau\rangle$ from 7.2 to 6.6 ns is observed.

The fluorescence anisotropy decay parameters of $N^{\epsilon B29}$-Abz-insulin are listed in Table 5. Fitting the data on the basis of a monoexponential model results in an enhancement of χ^2 with increasing w_0. This deterioration of the fits clearly indicates that at least two rotational correlation times are necessary to describe the anisotropy decays of the solubilized insulin. In Figure 8, an example of a biexponential fit of the data is given which results in a random distribution of the residuals. All rotational correlation times ϕ_2 measured in reversed micelles are long compared to the value of the monomeric species in aqueous solution (=2.3 ns) and are of the same order of magnitude at different w_0 values.

Table 4: Fluorescence Intensity Decay Parameters of $N^{\epsilon B29}$-Abz-Insulin in AOT (0.05 M)/*i*-Octane/Water, CTAB (0.05 M)/*i*-Octane/Trichloromethane (1/1; v/v)/Water, and DOcPC (0.05 M)/*i*-Octane/Hexanol (9/1; v/v)/Water, 25 mM_{wp} Tris, pH_{st} 7.8, as a Function of w_0[a]

w_0	B_1	B_2	B_3	τ_1 (ns)	τ_2 (ns)	τ_3 (ns)	$\langle\tau\rangle$ (ns)	χ^2
AOT Micelles								
3	0.03	0.68	0.29	1.26 ± 0.12	6.84 ± 0.16	9.96 ± 0.09	7.5	1.16
9	0.02	0.50	0.48	0.68 ± 0.18	6.58 ± 0.21	9.36 ± 0.05	7.8	1.09
20	0.02	0.58	0.40	0.73 ± 0.09	6.66 ± 0.17	9.80 ± 0.07	7.8	1.22
50	0.02	0.69	0.29	1.00 ± 0.06	7.02 ± 0.13	10.32 ± 0.09	7.8	1.11
CTAB Micelles								
3	0.02	0.33	0.65	0.73 ± 0.15	4.00 ± 0.11	7.35 ± 0.03	6.1	1.21
9	0.02	0.34	0.64	0.91 ± 0.23	4.66 ± 0.05	7.86 ± 0.08	6.6	1.20
20	0.09	0.63	0.28	1.07 ± 0.05	5.98 ± 0.09	10.11 ± 0.07	6.7	1.12
50	0.10	0.75	0.15	1.21 ± 0.04	6.55 ± 0.07	11.76 ± 0.13	6.8	1.29
DOcPC Micelles								
3	0.09	0.74	0.17	1.30 ± 0.05	6.80 ± 0.08	11.84 ± 0.13	7.2	1.14
9	0.08	0.55	0.37	1.02 ± 0.05	6.22 ± 0.13	10.39 ± 0.06	7.4	1.23
20	0.13	0.46	0.41	0.87 ± 0.03	5.12 ± 0.08	10.37 ± 0.05	6.7	1.28
50	0.16	0.45	0.39	0.94 ± 0.03	5.07 ± 0.08	10.70 ± 0.05	6.6	1.20

[a] Protein concentration, 1 μM; temperature, 22 °C; excitation wavelength, 330 nm; bandwidth, 16 nm; filter, KV 380; the lamp pulse was recorded at 410 nm. For further explanations, see legend to Table 1.

DISCUSSION

Structure in Aqueous Solution. Chemical conjugation of proteins with reporter groups for biochemical or biophysical studies is often accompanied by a disturbance of structural and/or functional properties of the molecule investigated. Therefore, in this study great importance has been attached to the demonstration that the properties of native insulin are not impaired by the Abz-label introduced in position B1 or conjugated with the ϵ-amino group of B29-lysine. Not only receptor binding capability and biopotency in vitro but also solution structure, according to CD spectroscopy, were shown to be largely the same as for the native hormone. Conformation and the propensity for self-association as well as the allosteric T→R transition in the hexameric state are not influenced by the covalently linked fluorophore which is distinguished by a nonbulky structure and a moderate hydrophobicity from most classical fluorescence labels.

Time-Resolved Fluorescence Measurements and Rotational Dynamics in Aqueous Solution. The spectral properties of Abz allow a selective excitation outside the spectral range of protein absorption. Furthermore, the Abz fluorescence is sensitive to solvent polarity and molecular environment. The similarities of the lifetime data of both insulin derivatives in the nonhexameric state correspond to the finding that the fluorophores are located in an environment of comparable polarity as indicated by the fluorescence emission maxima of 415 and 416 nm, respectively (see Table

Table 5: Fluorescence Anisotropy Decay Parameters of $N^{\epsilon B29}$-Abz-Insulin in AOT (0.05 M)/*i*-Octane/Water, CTAB (0.05M)/*i*-Octane/Trichloromethane (1/1; v/v)/Water, and DOcPC (0.05 M)/*i*-Octane/Hexanol (1/1; v/v)/Water, 25 mM_{wp} Tris, pH_{st} 7.8, as a Function of w_0[a]

w_0	r_0	r_1	r_∞	ϕ_1 (ns)	χ^2	r_0	r_1	r_2	r_∞	ϕ_1 (ns)	ϕ_2 (ns)	χ^2	α
						AOT Micelles							
3	0.305	0.282	0.023	8.3 ± 0.2	1.11	0.345	0.053	0.275	0.017	0.4 ± 0.4	9.1 ± 0.3	0.96	0.15
9	0.248	0.211	0.037	5.8 ± 0.2	1.56	0.276	0.070	0.180	0.026	1.1 ± 0.3	8.0 ± 0.4	1.15	0.25
20	0.218	0.178	0.040	4.7 ± 0.2	1.57	0.246	0.091	0.129	0.026	1.3 ± 0.3	8.4 ± 0.7	1.06	0.37
50	0.231	0.191	0.040	3.8 ± 0.2	2.90	0.288	0.142	0.123	0.023	0.9 ± 0.2	8.3 ± 0.6	1.24	0.49
						CTAB Micelles							
3	0.279	0.249	0.030	5.9 ± 0.2	1.18	0.288	0.133	0.155	0.000	3.1 ± 0.9	13.5 ± 0.3	1.00	0.46
9	0.254	0.219	0.035	3.5 ± 0.1	1.42	0.285	0.094	0.163	0.028	1.0 ± 0.3	5.2 ± 0.3	1.03	0.33
20	0.193	0.157	0.036	3.6 ± 0.2	1.32	0.229	0.089	0.113	0.027	0.8 ± 0.2	6.0 ± 0.5	0.90	0.39
50	0.197	0.165	0.032	2.9 ± 0.2	2.00	0.242	0.105	0.114	0.023	0.6 ± 0.1	5.1 ± 0.4	1.27	0.43
						DOcPC Micelles							
3	0.258	0.214	0.044	9.8 ± 0.4	1.24	0.355	0.115	0.207	0.033	0.2 ± 0.1	11.7 ± 0.5	0.99	0.32
9	0.225	0.189	0.036	7.6 ± 0.3	1.74	0.266	0.070	0.174	0.022	0.7 ± 0.3	10.7 ± 0.7	1.35	0.26
20	0.206	0.147	0.059	6.0 ± 0.3	1.77	0.365	0.195	0.130	0.040	0.1 ± 0.2	10.5 ± 0.7	1.08	0.53
50	0.172	0.112	0.060	3.5 ± 0.3	2.18	0.318	0.200	0.083	0.035	0.2 ± 0.1	11.9 ± 1.3	0.96	0.63

[a] Data analyses based on a monoexponential (left six columns) and biexponential model (right eight columns), respectively. Protein concentration, 1 μM; temperature, 22 °C. For further explanations, see legend to Table 2.

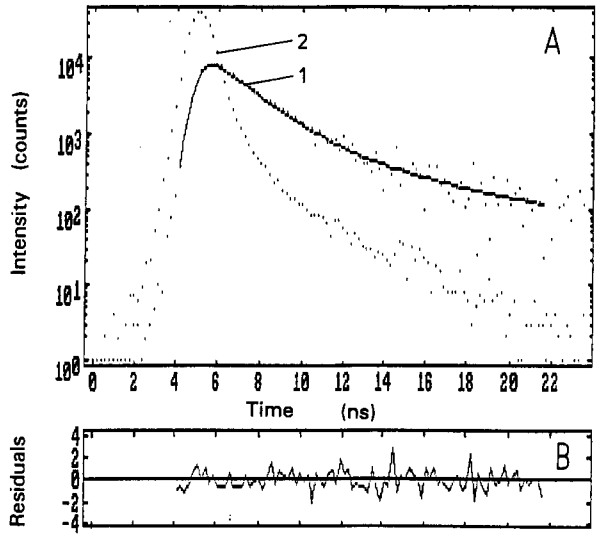

FIGURE 8: (A) Decay of the difference between vertical and horizontal polarization of $N^{\epsilon B29}$-Abz-insulin in AOT (0.05 M)/*i*-octane/water, 25 mM_{wp} Tris, at $w_0 = 9$ (1), curve fitting based on a biexponential model (line), and lamp pulse at 410 nm (2). (B) Residuals. 1 μM $N^{\epsilon B29}$-Abz-insulin; excitation at 330 nm, spectral bandwidth 16 nm; emission filter KV 380. $r_0 = 0.276$, $r_1 = 0.070$, $r_2 = 0.180$, $r_\infty = 0.026$, $\phi_1 = 1.1$ ns, $\phi_2 = 8.0$ ns, $\chi^2 = 1.15$.

1, rows 1 and 4). The appearance of up to three lifetimes (τ_i) indicates heterogeneity which is often found when evaluating fluorescence emission of proteins: For example, tryptophan and tyrosine residues show triple-exponential fluorescence intensity decays in the majority of cases, possibly due to the existence of rotamer/conformer populations with different fluorescence decay times [for more details, see, e.g., Willis and Szabo (1992)]. This explanation complies with the observation that for [Abz^{B1}]insulin the number of lifetimes is reduced to $i = 2$ when going from the monomer to the T_6 and R_6 hexamer and that the fluorescence of R_6 [Abz^{B1}]insulin is nearly monoexponential as judged by the ratio of amplitudes of 0.05/0.95. From a molecular point of view, the data reflect the involvement of the N-terminus of the B-chain in dimer−dimer contacts during hexamerization which should be accompanied by a more fixed orientation of the fluorophore. On principle, NMR spectroscopy is the most powerful method to prove such changes (Ross et al., 1992), but this clarification was not the aim of the present study.

The mean fluorescence lifetime of Abz, $\langle\tau\rangle = 8.4$ ns (Chen et al., 1967), is suitable for the measurement of rotational correlation times of globular proteins of a molecular mass of ≤80 kDa. Insulin is a molecule of molecular mass of 5.78 kDa and approximately spherical shape. According to the Stokes−Einstein relation, the rotational correlation time is related to the volume V of a rotating sphere, the viscosity η of the solution, the absolute temperature T, and the Boltzmann constant k by $\phi = \eta V/kT$. Using the equation $V_h = (M/N_L)(\langle v\rangle + h)$ which relates the hydrodynamic volume V_h of a protein to its molecular mass M, specific volume $\langle v\rangle$, and hydration h (Yguerabide et al., 1970), the calculated rotational correlation times are 2.1 and 12.4 ns in the monomeric and hexameric state, respectively, and, hence, are commensurable with the mean fluorescence lifetime of the label. This commensurability complies with the prerequisite of a reliable determination of the rotational dynamics of the labeled insulins in solution.

The rotational correlation times of 2.3 and 2.5 ns of $N^{\epsilon B29}$-Abz-insulin and [Abz^{B1}]insulin, respectively, are coincident with the existence of monomers at a concentration of 0.3−0.4 μM (see Table 2); however, the low limiting anisotropies of 0.204 and 0.233 compared to 0.304 of the free label (Haugland & Stryer, 1967) are indicative of an unresolved fast side-chain mobility. When going to the hexameric state which is characterized by a compact packing of the subunits to an oblate spheroid with a diameter of about 5.0 nm and a height of about 3.5 nm according to the crystal structure (Blundell et al., 1972), the prolongation of the rotational correlation times means an increase of the hydrodynamic radii of the monomers from 1.34 and 1.37 nm to 2.24 and 2.44 nm of the 2Zn-hexamers measured for the T_6 state of $N^{\epsilon B29}$-Abz-insulin and [Abz^{B1}]insulin, respectively. As mentioned above, the N-terminal B-chain residues are involved in dimer−dimer contacts. Especially residue B1 is fitted into a pocket between the A main chain and A14-tyrosine residue of its neighbour (Baker et al., 1988). This involvement of position B1 in quaternary contacts of the hexamer is reflected not only in the lifetime data (Table 1) but also in the higher r_0 values as well as lower ratios α of [Abz^{B1}]insulin both in the T_6 and in the R_6 state, indicating a higher motional

Table 6: Inner and Outer Radii, r_c and r_h, Respectively, and the Corresponding Rotational Correlation Times, ϕ_m, of Reversed Micelles of AOT in *i*-Octane/Water and CTAB in *i*-Octane/Hexanol (9/1; v/v)/Water at 25 °C According to Vos et al. (1987)

micelle	w_0	r_c (nm)	r_h (nm)	ϕ_m (ns)
AOT	5	1.2	2.4	7
AOT	10	1.7	2.9	12
AOT	20	3.4	4.6	47
AOT	50	6.7	7.9	238
CTAB	5			
CTAB	10	1.9	4.3	41
CTAB	20	3.1	5.5	85
CTAB	50	6.3	8.7	335

restriction of the label at the N-terminus of the B-chain compared to the C-terminus of $N^{\epsilon B29}$-Abz-insulin, where the label is located on the polar surface of the hexamer. In the T_6 state of [Abz^{B1}]insulin, the experimental value of r_0 equals the limiting anisotropy of the Abz fluorophore given in the literature and indicates that there is no unresolved motional mobility. The long correlation time, ϕ_2, is in accordance with the calculated radius of 2.34 nm of the insulin hexamer based on the hydrodynamic theory, while ϕ_1 is in the range typical of side-chain mobility (Munro et al., 1979). High mobility of the side chain at the C-terminus of the B-chain is even preserved in the hexameric state of $N^{\epsilon B29}$-Abz-insulin as deducible from the low value of r_0, and an incomplete resolution of the overall rotational motion of the hexamer and side-chain mobility is responsible for the slight difference between ϕ_2 of $N^{\epsilon B29}$-Abz-insulin in the T_6 state and the respective value of [Abz^{B1}]insulin.

Transformation of the hexamers of both labeled insulins from the T to the R state, which is accompanied by a change in conformation of the first eight residues of the B-chain from extended to α-helical (Bentley et al., 1976; Smith et al., 1984), shortens the overall rotational correlation times, indicating that the allosteric transition in solution results in a more compact packing of the subunits in the R_6 state compared to the T_6 state. This is confirmed by the reduction of α. It is a feature of the fluorophore chosen that such a slight change of the hydrodynamic properties of the hexamer can be monitored.

Structure in Reversed Micelles. Before discussing structural aspects of insulin solubilized in reversed micelles, it is worthwhile to make some considerations on micellar dimensions and concentrations to demonstrate the special properties of microstructured systems which distinguish such systems from aqueous solution.

Beside the high optical transparency of the AOT/*i*-octane/water system, an important feature of this ternary system is that AOT micelles display a narrow size distribution; micellar size itself is dependent on the water/amphiphile ratio. Regarding a reversed micellar system of AOT in *i*-octane at a constant AOT concentration of 0.05 M, the mean aggregation number increases with increasing water concentration, and the micellar inner core radii r_c vary from 1.2 nm at w_0 = 5 to 6.7 nm at w_0 = 50 (see Table 6).

On the basis of an overall protein concentration of 100 μM on which the CD experiments were typically carried out, the number of micelles exceeds by far the number of protein molecules at low w_0, whereas at w_0 = 35 a nearly stoichiometric micelle/protein ratio exists as deduced from the mean apparent molecular weight of AOT aggregates given in the literature (Eicke & Kvita, 1984). Especially in the case of proteinaceous solubilizates, which—like insulin—are insoluble in alkanes, it is logical to relate the concentrations of solubilizates to the micellar water. These water pool concentrations are drastically higher than those related to the bulk medium as shown by the following example: An overall insulin concentration of 100 μM in a 0.5 M AOT solution in *i*-octane corresponds to endomicellar concentrations c_{wp} of 12 mM (69 g/L) and 3.2 mM (18 g/L) at w_0 = 9 and w_0 = 35, respectively. These aspects are of great importance when looking at the quaternary structure of insulin which, in aqueous solution, is highly dependent on its concentration. In the following, the results of the CD as well as fluorescence spectroscopic studies will be discussed against the background of these formal considerations.

In AOT reversed micelles, the far-UV CD spectra of native insulin and the labeled insulins are typical of proteins with a substantial content of helical structure. In the crystalline state, the conformation of rhombohedral 2Zn-insulin is composed of 51% α-helix, 14% antiparallel β-structure, about 14% turn, and 21% aperiodic structure. The profiles of the CD spectra measured in reversed micelles are similar to those of insulin and insulin derivatives when monomeric due to high dilution (Wood et al., 1975) or to the absence of the C-terminal residues B26−B30 (Fischer et al., 1985), and are absolutely different from those measured after denaturation by, e.g., guanidinium chloride (Brems et al., 1990; Mullican & Brems, 1994). The computational analyses of the spectra according to Provencher and Glöckner (1981) agree well with the analyses according to Johnson (1990). At w_0 = 9, the α-helix content of the solubilized insulins is about 38% and is of the order of magnitude found for insulin in aqueous solution. With increasing micellar size, the α-helix content of the solubilized insulins slightly decreases.

In contrast to the CD spectra in the far-UV, the near-UV CD spectra are markedly affected in reversed micelles compared to aqueous solution. The increase of the negative ellipticity at 253 nm is indicative of an alteration of the disulfide dihedral angles (Beychok, 1965; Linderberg & Michl, 1970), which is also measured during the T→R transition of insulin (Renscheidt et al., 1984; Wollmer et al., 1987). The weak CD in the absorption range of tyrosine is characteristic of reduced aromatic interactions, which may be attributed to a reorientation or enhanced mobility (Jirgensons & Capitello, 1970) of the aromatic side chains in the micellar environment. Interestingly, the near-UV CD of the inherently achiral fluorescence label 2-aminobenzoic acid is dependent on the position in the protein: The label exhibits intensive Cotton effects only in position B1, while the extrinsic chromophore covalently linked to the C-terminus of the B-chain does not show any dichroic band. This observation implies that the tertiary contacts of the Abz residue existing in aqueous solution are not completely abolished in reversed micelles, but are more or less pronounced depending on the position within the protein.

In conclusion, the CD spectra of the solubilized insulins in the far- and near-UV region reveal the same shape as found for proteins in an intermediate state of folding which was described as "compact globule with native-like secondary structure and with slowly fluctuating tertiary structure" after characterization on CD spectroscopic grounds by

Dolgikh et al. (1981). Later, this kind of folding intermediate was referred to as the "molten globule" (Ohgushi & Wada, 1983), and it has been shown that this state of folding can be induced, for instance, by denaturing agents, by varying the pH (especially at low pH), or, notably, by high ionic strength (Stigter et al., 1991) as present in AOT micelles. In the scope of structural insulin biochemistry, the existence of a molten globule state was first postulated for the monomeric des-(B26−B30)-insulin in 20 vol % aqueous acetic acid by Hua et al. (1992b). In that study, the observed NOESY spectrum of des-(B26−B30)-insulin contained fewer tertiary contacts than predicted on the basis of its crystal structure, whereas slowly exchanging amide resonances in ^2H_2O were characteristic of a native-like, rather rigid secondary structure.

The reduced aromatic interactions in reversed micelles comply with the finding that, in spite of the high protein concentration related to micellar water, the formation of quaternary structure can be ruled out CD spectroscopically. Specific protein−protein interactions in reversed micelles are, however, possible on principle (Groome et al., 1990) as also shown by the enzymatic hydrolysis of a fluorogenic insulin derivative and of native insulin by serine proteases solubilized in AOT or CTAB micelles (Lenz et al., 1994).

Fluorescence Measurements and Rotational Dynamics in Reversed Micelles. According to Figure 7A,B, the polarity of the environment of the fluorophores increases in the range $2 \leq w_0 \leq 20$ and remains approximately constant at $w_0 > 20$. Correspondingly, substantial changes are observed for the lifetimes, their amplitudes, and $\langle\tau\rangle$ values when w_0 is increased from 3 to 9 and from 9 to 20, but not from 20 to 50 (Table 4). The shortening of the lifetimes compared to those of the monomeric *N*-Abz-insulin in aqueous solution (Table 1, row 1) indicates dynamic quenching by the polar head groups of the amphiphiles, and the variation of the lifetime amplitudes shows that the dynamics of the fluorophore are affected by the micellar environment. Compared to aqueous solution, small differences consistently remain even at $w_0 = 50$.

Reversed micelles can be assumed to be perfect rotating spheres, and their radii can be calculated on the basis of their rotational correlation times according to the Stokes−Einstein relation (Bucci & Steiner, 1988). The measured rotational correlation times and corresponding radii of AOT and CTAB reversed micelles are given in Table 6. The values for DOcPC reversed micelles are not described in the literature, however, the results of the FAD measurements are still presented in order to show that the findings in anionic, cationic, and zwitterionic amphiphiles are qualitatively the same. As demonstrated by CD spectroscopy, quaternary interactions of the insulins in AOT micelles can be ruled out, and, concerning the FAD measurements, the solubilized insulins will hence be regarded as monomeric in the solvent systems investigated.

In aqueous solution, the fluorescence anisotropy decay of the monomeric insulins had to be fitted with two rotational correlation times, with the shorter attributable to side-chain mobility and the longer to the overall rotation of the protein. If the rotational motion of the solubilizate and the rotation of the hosting micelle are regarded as independent of each other, the anisotropy decays can be described by the following equation:

$$r(t) = [r_s \exp(-t/\phi_s) + r_p \exp(-t/\phi_p)]r_m \exp(-t/\phi_m)$$

$$r(t) = r_1 \exp[-t(1/\phi_s + 1/\phi_m)] + r_2 \exp[-t(1/\phi_p + 1/\phi_m)]$$

$$r(t) = r_1 \exp(-t/\phi_1) + r_2 \exp(-t/\phi_2)$$

$$\Rightarrow 1/\phi_2 = 1/\phi_p + 1/\phi_m \quad (1)$$

The index s denotes side-chain mobility, p the rotation of the protein, and m the rotation of the micelle. Since ϕ_m is known from the literature (see Table 6), and the values of ϕ_2 were determined in this study (Table 5), it is possible to calculate ϕ_p, the rotational correlation time of the protein within the micelle. The calculated values of ϕ_p are listed in Table 7. This analysis model resolves the superposition of the rotational movement of the protein and the rotation of the hosting micelle.

In the AOT system, the mobility of insulin within the micelle is reduced with decreasing w_0 ($\phi_p \rightarrow \infty$) until $\phi_2 = \phi_m$: At $w_0 = 3$, the Stokes−Einstein calculation of the outer micellar radius with ϕ_2 results in 2.7 nm for AOT micelles hosting $N^{\epsilon B29}$-Abz-insulin when the viscosity of the bulk solvent is taken into account (Vos et al., 1987). Indeed, the radius of the filled AOT micelle is larger than the radius of the empty micelle (see Table 6) and amounts nearly to the sum of the hydrodynamic radius of insulin of 1.3 nm and the mean length of one AOT molecule of 1.2 nm (Zulauf & Eicke, 1979). With increasing w_0, ϕ_p (Table 7) and r_0 (Table 5, right column) decrease, while α increases: The data reveal that the swelling of the micelles is accompanied by an enhancement of the mobility of the hosted protein. This result clearly proves that the labeled insulin is not integrated into the amphiphile monolayer.

Assuming that DOcPC micelles also possess a spherical shape and swell with increasing water/amphiphile ratio, the results of the FAD measurements are qualitatively in accordance with those obtained with AOT micelles.

In the case of cationic CTAB micelles, however, ϕ_2 changes with w_0, whereas ϕ_p and α do not significantly. The internal mobility is high over the whole range of w_0, and a similar calculation at $w_0 = 3$ as performed for AOT micelles (see above) is not possible because of the high remaining mobility of the insulin molecule. Nevertheless, the rotational motion is somewhat reduced in comparison to the insulin monomer in aqueous solution.

In conclusion, the time-resolved FAD measurements show that the labeled insulins are not integrated into the amphiphile monolayers of reversed micelles, but that there exist amphiphile−protein interactions which, especially in small micelles, can result in a strong immobilization of the solubilized proteins. However, the rotational dynamics are slowed down even in large micelles compared to aqueous solution. In this respect, the anionic amphiphile AOT interacts in a stronger way with the insulin derivate than the cationic CTAB.

General Aspects of Amphiphile−Insulin Interactions. In this work, studies on the solution structure of insulin were extended to reversed micellar solvent systems mimicking the lipid−water interface of biological membranes, and the existence of remarkable amphiphile−insulin interactions in reversed micelles was demonstrated by the observation that

Table 7: Calculated Internal Rotational Correlation Times, ϕ_p, of $N^{\epsilon B29}$-Abz-Insulin in AOT and CTAB Micelles as a Function of w_0[a]

micelle	w_0	ϕ_p (ns)
AOT	9	24.3
AOT	20	10.3
AOT	50	8.6
CTAB	9	5.9
CTAB	20	6.5
CTAB	50	5.2

[a] ϕ_p was calculated according to eqn 1: $1/\phi_2 = 1/\phi_p + 1/\phi_m$. For the calculation, values of ϕ_2 and ϕ_m are taken from Tables 5 and 6, respectively.

labeled insulin can be immobilized with respect to the motion of the hosting micelle. Since insulin is a ligand of a transmembrane receptor, interactions of insulin with lipids of the plasma membrane similar to these observed in the biomimetic systems of this study and controlled by the lipid pattern of the membrane may occur during its biological pathway and may be related to the finding that insulin action is characterized by cell specificity (Linde et al., 1981; Sonne et al., 1983; Gammeltoft, 1984). Furthermore, the results of this study show that reversed micellar insulin exhibits extraordinary structural features which are—according to CD spectroscopy—typical of proteins in the molten globular state, an intermediate state of folding and unfolding which was formerly supposed and later shown to be involved in membranal processes of proteins (Bychkova et al., 1988; van der Goot et al., 1991) and which was proposed to be of relevance for the receptor ligation especially in the case of insulin according to the hypothesis of Hua et al. (1992).

The importance of the observed and reported phenomena of this study for the situation in vivo is an open question, but the evident influence of charged amphiphiles on insulin structure in solution underlines the conformational variability of the monomer (Burke et al., 1990; Nakagawa & Tager, 1993; Hua et al., 1991) which further investigations should be focused on, not only to gain further insight on how conformation and quaternary structure of bioactive proteins are modulated by a membranal environment but also with respect to the possible relevance of lipid–protein interactions for the mechanism of insulin action.

ACKNOWLEDGMENT

We particularly thank Prof. Dr.-Ing. Dr. h.c. mult. H. Zahn for his interest in this study. Furthermore, we thank Dr. J. Föhles, Hubert Mohr, and Manfred Dewor for performing the amino acid analyses, and Cornelia Diaconescu and Josef Tenelsen for the results of the biological studies. Thanks are due to Margot Leithäuser, Konstanze Thiemann, and Jürgen Stahl for their excellent technical assistance.

REFERENCES

Ahlers, M., Müller, W., Reichert, A., Ringsdorf, H., & Venzmer, J. (1990) *Angew. Chem. 102*, 1310–1327.

Baker, E. N., Blundell, T. L., Cutfield, J. F., Cutfield, S. M., Dodson, E. J., Dodson, G. G., Crowfoot Hodgkin, D. M., Hubbard, R. E., Isaacs, N. W., Reynolds, C. D., Sakabe, K., Sakabe, N., & Vijayan, N. M. (1988) *Philos. Trans. R. Soc. London, B 319*, 369–456.

Bentley, G. A., Dodson, E. J., Dodson, G. G., Hodgkin, D., & Mercola, D. (1976) *Nature 261*, 166–168.

Beychok, S. (1965) *Proc. Natl. Acad. Sci. U.S.A. 53*, 999–1006.

Blundell, T., Dodson, G., Hodgkin, D., & Mercola, D. (1972) *Adv. Protein Chem. 26*, 279–402.

Brems, D. N., Brown, P. L., Heckenlaible, L. A., & Frank, B. H. (1990) *Biochemistry 29*, 9289–9293.

Bucci, E., & Steiner, R. F. (1988) *Biophys. Chem. 30*, 199–224.

Burke, G. T., Hu, S. Q., Ohta, N., Schwartz, G. P., Zong, L., & Katsoyannis, P. G. (1990) *Biochem. Biophys. Res. Commun. 173*, 982–986.

Bychkova, V. E., Pain, R. H., & Ptitsyn, O. B. (1988) *FEBS Lett. 238*, 231–234.

Chapman, D., Comez-Fernandez, J. C., & Goni, F. M. (1979) *FEBS Lett. 98*, 211–223.

Chen, G. C., & Yang, J. T. (1977) *Anal. Lett. 10*, 1195–1207.

Chen, R. F., Vurek, G. G., & Alexander, N. (1967) *Science 156*, 949–951.

De Meyts, P. (1976) *Methods Mol. Biol. (N.Y.) 9*, 301–383.

Derewenda, U., Derewenda, Z., Dodson, E. J., Dodson, G. G., Reynolds, C. D., Smith, G. D., Sparks, C., & Swenson, D. (1989) *Nature 338*, 594–596.

Dolgikh, D. A., Gilmanshin, R. I., Brazhnikov, E. V., Bychkova, V. E., Semisotnov, G.V., Venyaminov, S. Y., & Ptitsyn, O. B. (1981) *FEBS Lett. 136*, 311–315.

Doub, L., & Vandenbelt, J. M. (1949) *J. Am. Chem. Soc. 71*, 2414–2420.

Eicke, H. (1980) *Top. Curr. Chem. 87*, 85–145.

Eicke, H.-F., & Kvita, P. (1984) in *Reversed Micelles—Biological and Technological Relevance of Amphiphilic Structures in Apolar Media* (Luisi, P. L., & Straub, B. E., Eds.) pp 21–35, Plenum Press, New York and London.

Ekwall, P., Mandell, L., & Fontell, K. J. (1969) *J. Colloid Interface Sci. 29*, 639.

Federwisch, M. (1993) Doctoral Thesis, RWTH Aachen.

Federwisch, M., Casaretto, M., Gerardy-Schahn, R., Bitter-Suermann, D., & Wollmer, A. (1992) *Biophys. Chem. 44*, 151–161.

Fendler, J. H. (1982) *Membrane mimetic chemistry*, John Wiley & Sons, Inc., New York.

Finney, D. J. (1964) in *Statistical Methods in Biological Analysis*, 2nd ed., Charles Griffin & Co. Ltd., London.

Fischer, W. H., Saunders, D., Brandenburg, D., Wollmer, A., & Zahn, H. (1985) *Biol. Chem. Hoppe-Seyler 366*, 521–525.

Frank, B. H., & Veros, A. J. (1968) *Biochem. Biophys. Res. Commun. 32*, 155–160.

Gammeltoft, S. (1984) *Physiol. Rev. 64*, 1321–1378.

Geiger, R., Obermeier, R., & Tesser, G. I. (1975) *Chem. Ber. 108*, 2758–2763.

Gray, W. R., & Hartley, B. S. (1963) *Biochem. J. 89*, 59P.

Groome, N. P., Vacher, M., Nicot, C., & Waks, M. (1990) *Biochem. Int. 21*, 1–7.

Haugland, R. P., & Stryer, L. (1967) in *Conformation of Biopolymers* (Ramachandran, G. N., Ed.) Vol. 1, pp 321–335, Academic Press, London and New York.

Hua, Q. X., Shoelson, S. E., Kochoyan, M., & Weiss, M. A. (1991) *Nature 354*, 238–241.

Hua, Q. X., Shoelson, S. E., & Weiss, M. A. (1992a) *Biochemistry 31*, 11940–11951.

Hua, Q. X., Kochoyan, M., & Weiss, M. A. (1992b) *Proc. Natl. Acad. Sci. U.S.A. 89*, 2379–2383.

Inokuti, M., & Hirayama, F. (1965) *J. Phys. Chem. 43*, 1978–1989.

Jirgensons, B., & Capitello, S. (1970) *Biochim. Biophys. Acta 214*, 1–5.

Johnson, W. C., Jr. (1990) *Proteins: Struct., Funct., Genet. 7*, 205–214.

Kaarsholm, N. C., Ko, H.-C., & Dunn, M. F. (1989) *Biochemistry 28*, 4427–4435.

Lakowicz, J. R. (1986) *Methods Enzymol. 131*, 518–567.

Lenz, V. J., Gattner, H.-G., Leithäuser, M., Brandenburg, D., Wollmer, A., & Höcker, H. (1994) *Anal. Biochem. 221*, 85–93.

Linde, S., Sonne, O., Hansen, B., & Gliemann, J. (1981) *Hoppe-Seyler's Z. Physiol. Chem. 362*, 573–579.

Linderberg, J., & Michl, J. (1970) *J. Am. Chem. Soc. 92*, 2619–2625.

Luisi, P. L. (1985) *Angew. Chem. 97*, 449–460.

Martin, C. A., & Magid, L. J. (1981) *J. Phys. Chem. 85*, 3938–3944.

Menger, F. M., Donohue, J. A., & Williams, R. F. (1973) *J. Am. Chem. Soc. 95*, 286−288.
Moody, A. J., Stan, M. A., Stan, M., & Gliemann, J. (1974) *Hormone Metab. Res. 6*, 12−16.
Moroder, L., Hallet, A., Wünsch, E., Keller, O., & Wersin, G. (1976) *Hoppe-Seyler's Z. Physiol. Chem. 357*, 1651−1653.
Mullican, R. L., & Brems, D. N. (1994) *Biochemistry 33*, 1116−1124.
Munro, I., Pecht, I., & Stryer, L. (1979) *Proc. Natl. Acad. Sci. U.S.A. 76*, 56−60.
Nakagawa, S. H., & Tager, H. S. (1993) *Biochemistry 32*, 7237−7243.
Nicot, C., Vacher, M., Vincent, M., Gallay, J., & Waks, M. (1985) *Biochemistry 24*, 7024−7032.
Ohgushi, M., & Wada, A. (1983) *FEBS Lett. 164*, 21−24.
Provencher, S. W., & Glöckner, J. (1981) *Biochemistry 20*, 33−37.
Renscheidt, H., Strassburger, W., Glatter, U., Wollmer, A., Dodson, G. G., & Mercola, D. A. (1984) *Eur. J. Biochem. 142*, 7−14.
Ringsdorf, H., Schlarb, B., & Venzmer, J. (1988) *Angew. Chem. 100*, 117−162.
Ross, J. B. A., Wyssbrod, H. R., Porter, R. A., Schwartz, G. P., Michaels, C. A., & Laws, W. R. (1992) *Biochemistry 31*, 1585−1594.
Sargent, D. F., & Schwyzer, R. (1986) *Proc. Natl. Acad. Sci. U.S.A. 83*, 5774−5778.
Schüttler, A. (1979) Doctoral Thesis, RWTH Aachen.
Smith, G. D., Swenson, D. C., Dodson, E. J., Dodson, G. G., & Reynolds, C. D. (1984) *Proc. Natl. Acad. Sci. U.S.A. 81*, 7093−7097.
Sonne, O., Linde, S., Larsen, T. R., & Gliemann, J. (1983) *Hoppe-Seyler's Z. Physiol. Chem. 364*, 101−110.
Spackman, D. H., Stein, W. H., & Moore, S. (1958) *Anal. Chem. 30*, 1190−1206.
Stigter, D., Alonso, D. O. V., & Dill, K. A. (1991) *Proc. Natl. Acad. Sci. U.S.A. 88*, 4176−4180.
Sui, S., Urumow, T., & Sackman, E. (1988) *Biochemistry 27*, 7463−7469.
Szabo, A. G., & Rayner, D. M. (1980) *J. Am. Chem. Soc. 102*, 554−563.
Van der Goot, F. G., González-Mañas, J. M., Lakey, J. H., & Pattus, F. (1991) *Nature 354*, 408−410.
Vos, K., Laane, C., Weijers, S. R., van Hoek, A., Veeger, C., & Visser, A. J. W. G. (1987) *Eur. J. Biochem. 169*, 259−268.
Willis, K. J., & Szabo, A. G. (1992) *Biochemistry 31*, 8924−8931.
Wollmer, A., Rannefeld, B., Johansen, B. R., Hejnaes, K. R., Balschmidt, P., & Hansen, F. B. (1987) *Biol. Chem. Hoppe-Seyler 368*, 903−911.
Wood, S. P., Blundell, T. L., Wollmer, A., Lazarus, N. R., & Neville, R. (1975) *Eur. J. Biochem. 55*, 531- 537.
Wu, C.-S. C., & Yang, J. T. (1981) *Biochim. Biophys. Acta 667*, 285−293.
Yguerabide, J., Epstein, H. F., & Stryer, L. (1970) *J. Mol. Biol. 51*, 573−590.
Zulauf, M., & Eicke, H. F. (1979) *J. Phys. Chem. 83*, 480−486.

BI9423594